WATER RESEARCH 44 (2010) 1270–1278

Available at www.sciencedirect.com

journal homepage: www.elsevier.com/locate/watres

Colloid transport with wetting fronts: Interactive effects of solution surface tension and ionic strength

Jie Zhuang [a,*], *Nadine Goeppert* [b], *Ching Tu* [c], *John McCarthy* [c], *Edmund Perfect* [c], *Larry McKay* [c]

[a] *Institute for a Secure and Sustainable Environment, Department of Biosystems Engineering and Soil Science, The University of Tennessee, Knoxville, TN 37996-4134, United States*

[b] *Department of Environmental Sciences and Energy Research, Weizmann Institute of Science, 76100 Rehovot, Israel*

[c] *Department of Earth and Planetary Sciences, Center for Environmental Biotechnology, The University of Tennessee, Knoxville, TN 37996, United States*

ARTICLE INFO

Article history:
Received 5 June 2009
Received in revised form
20 November 2009
Accepted 9 December 2009
Available online 23 December 2009

Keywords:
Colloid transport
Transient unsaturated flow
Surface tension
Ionic strength
Horizontal column
Capillary force

ABSTRACT

Transport of colloids with transient wetting fronts represents an important mechanism of contaminant migration in the vadose zone. The work presented here used steady-state saturated and transient unsaturated flow columns to evaluate the transport of a fluorescent latex microsphere (980 nm in diameter) with capillary wetting fronts of different solution surface tensions and ionic strengths. The saturated transport experiments demonstrated that decreasing solution surface tension and ionic strength decreased colloid deposition at the solid-liquid interface and increased colloid recovery in the column effluent. The effect of solution surface tension on colloid transport and deposition was greater at lower ionic strength, suggesting an interaction between these two factors. Under transient unsaturated flow conditions, the number of colloids retained in sand decreased exponentially with travel distance through the porous media. However, lowering the solution surface tension and ionic strength resulted in a more even distribution of colloids along the column. The measured zeta potentials of colloids in different solutions suggest that both lowering surface tension and ionic strength would enhance the electrostatic repulsion between colloid and sand. The experimental results revealed that the effects are nonlinear, implying the possible existence of critical threshold values, beyond which the effects were not significant. In addition, colloid migration slowed down as solution surface tension decreased due to reduction of capillary forces that drove liquid movement.

1. Introduction

Colloid transport in the subsurface is of concern to drinking water quality due to introduction of viruses, pathogenic bacteria, protozoans, and colloid-/nano-sized industry materials, as well as the potential for co-transport of toxic chemicals sorbed to mobile mineral colloids (McCarthy and Zachara, 1989; Kretzschmar et al., 1999; McCarthy and McKay, 2004; DeNovio et al., 2004). More than 2000 articles have been published to address colloid transport, but the vast majority of the studies focused on water-saturated (groundwater) environments, even though most pathogens and toxicants enter groundwater via transport through the vadose zone, i.e., the shallow zone only partially saturated with water. Further, almost all studies of unsaturated systems are limited to steady-state flow, while in nature flow in the vadose zone is

* *Corresponding author*. Tel.: +1 865 974 1325; fax: +1 865 974 1838.
E-mail address: jzhuang@utk.edu (J. Zhuang).

0043-1354/$ – see front matter © 2009 Elsevier Ltd. All rights reserved.
doi:10.1016/j.watres.2009.12.012

dominated by alternate transient wetting and drying events (e.g., rainfall, drainage, and evaporation). Under steady-state flow conditions, air–water and air–water–solid interfaces are relatively stable and uniformly distributed in soil, resulting in persisting attachment of colloids at those interfaces (Wan and Wilson, 1994; Wan and Tokunaga, 2002; Zhuang et al., 2005). However, under transient unsaturated flow conditions, the transport is subject to temporal changes in water content and pore water velocity and thus in the thickness of water films and connectivity of flow paths. Movement of the air–water interface and the configuration and connectivity of air–water–solid interfaces have been found to promote colloid detachment and transport (Leenaars and O'Brien, 1989; Noordmans et al., 1997; Gomez-Suarez et al., 1999; El-Farhan et al., 2000; Saiers, 2003; Saiers et al., 2003; Gao et al., 2006; Shang et al., 2008). Expansion of water film and increase in pore saturation at the beginning of infiltration cause colloid release from the interfaces, and likewise shrinking water film during drainage pulls colloids to move with the desaturation (or drying) front (Saiers and Lenhart, 2003; Crist et al., 2004, 2005; Zhuang et al., 2007, 2009). Field studies demonstrate that soil colloids can be released in large concentrations during rainfall events, presumably due to hydrodynamic and chemical perturbations associated with the advancing wetting front (Kaplan et al., 1993; Ryan et al., 1998; Jarvis et al., 1999; Worrall et al., 1999; El-Farhan et al., 2000). Water content/pressure and capillary forces have been reported to play a significant role during transient flow in controlling interfacial retention and transport of colloids (Gao et al., 2008; Shang et al., 2008). These studies and others have greatly improved our understanding of the transient process of colloid transport (Ryan and Elimelech, 1996; Swartz and Gschwend, 1998; DeNovio et al., 2004). However, colloid transport with capillary wetting front and its dependence on solution conditions (e.g., chemistry and surface tension) have not been well examined.

In the presence of an anionic surfactant, zeta potential of colloids increases while the van der Waals attraction between colloid and surface decreases, resulting in increased repulsion and colloid release (Batra et al., 2001). A few studies have indicated that surfactant-induced reduction in surface tension could decrease the capillary pressure in unsaturated porous media, suggesting that surfactant enhanced drainage as a result of decreased surface tension (Zartman and Bartsch, 1990; Walker et al., 1998; Jawitz et al., 1998; Henry et al., 1999; Smith and Gillham, 1999). The effects of surface-active solutes on unsaturated flow and transport have also been seen in two-dimensional laboratory experiments on the transport and remediation of light non-aqueous phase liquid (Chevalier, 2003). Surface tension forces induced by passage of air–liquid interfaces (e.g., injection of air bubbles) have been observed to be effective in detaching colloids that are attached on matrix surface (Leenaars and O'Brien, 1989; Noordmans et al., 1997; Boks et al., 2008). All these studies demonstrated the potential that surface-active aqueous solutions (e.g., alcohols, humic substances, aliphatics, aromatics, and commercial surfactants), which have low surface tensions, may impact the retention, transport, and remobilization of colloids and colloid-associated contaminants (Henry and Smith, 2002). However, few studies have examined the surface tension effect under transient unsaturated flow conditions, particularly its interactions with the effect of solution ionic strength. The objective of this study was to determine colloid transport in porous media with capillary wetting front in solutions of varying surface tensions and ionic strengths. The coupled effects of ionic strength and surface tension were evaluated in terms of deposition rate, variation of colloid concentration with infiltration distance, and travel time.

2. Materials and method

2.1. Porous medium and experimental solution

A summary of the experimental conditions maintained for the columns is provided in Table 1. The porous material used for the transport experiments was a silica sand with a trade name Accusand (grade 50/70, Unimin Corporation, New Canaan, CT, USA). The sand grains had a median diameter (d_{50}) of

Table 1 – Summary of the conditions of column experiments.

Exp. #	Flow condition	Ionic strength (mM)	Surface tension (mN m^{-1})	Bulk density (g cm^{-3})	Porosity	Pore velocity (cm min^{-1})
1	saturated	2	73	1.79	0.34	5.55
2	saturated	5	73	1.82	0.33	6.07
3	saturated	10	73	1.83	0.32	6.13
4	saturated	20	73	1.84	0.32	5.83
5	saturated	50	73	1.82	0.33	5.86
6	saturated	2	30	1.83	0.32	6.09
7	saturated	5	30	1.83	0.32	5.98
8	saturated	10	30	1.83	0.32	6.50
9	unsaturated	2	73	1.82	0.33	varying
10	unsaturated	20	73	1.81	0.33	varying
11	unsaturated	50	73	1.83	0.32	varying
12	unsaturated	2	54	1.86	0.31	varying
13	unsaturated	2	46	1.86	0.31	varying
14	unsaturated	2	30	1.85	0.31	varying
15	unsaturated	50	46	1.83	0.32	varying
16	unsaturated	50	30	1.84	0.32	varying

0.25 ± 0.01 mm. Prior to the experiments, the sand was first washed with tap water until the rinse water was free of suspended impurities, and then reacted with 6 M HNO_3 for 5 h at 80 °C to remove metal oxides from the grain surfaces. After the treatments, the acid was decanted, and the sand was thoroughly rinsed with deionized water. To ensure that the sand was free of metal oxides, the sand was further treated following a procedure modified from the method of Mehra and Jackson (1960), which is described briefly here. Five hundred-mL 0.2 M citrate buffer solution that contained 44.1 g L^{-1} sodium citrate ($Na_3C_6H_5O_7 \cdot 2H_2O$) and 10.5 g L^{-1} citric acid ($C_6H_8O_7$) was added to a 2-L polyethylene bottle containing 300 g of the HNO_3-treated sand. The bottle was put in a shaking water bath (120 rpm) maintained at a temperature of 80 °C where 15 g of sodium dithionite ($Na_2S_2O_4$) was added to the bottle. The bottle was removed from the shaker and hand-shaken thoroughly for several seconds, then returned to the shaker and vigorously shaken for 1 min. Next, the speed was reduced and the sample was digested for 15 min with occasional vigorous shaking. The solution was decanted from the sand and the procedure was repeated three additional times. Finally the sand was rinsed with deionized water until the electric conductivity of the water reached near zero. The main drying curve of the water characteristic function was measured for the sand with a Tempe pressure cell (Soil Moisture Equipment Inc., Model 1400B0.5M2-3) (Dane and Hopmans, 2002) at bulk density of 1.82 g cm^{-3}, and parameterized using the van Genuchten (1980) equation, yielding $\theta = 0.332[1 + (0.074\psi)^{8.47}]^{-0.882} + 0.003$ ($R^2 = 0.96$), where θ is the volumetric water content ($m^3\ m^{-3}$) and ψ is the absolute value of soil water potential in cm of H_2O.

The experimental background solution was deaerated $NaNO_3$ solution (pH 7) of varying ionic strengths and concentrations of 2-propanol for different experimental purposes. The experimental ionic strengths ranged from 2 mM to 50 mM. Solution of 2-propanol was used to create low surface tension solutions. The resulting surface tensions were 30 mN m^{-1}, 46 mN m^{-1}, and 54 mN m^{-1} when the fractions of 2-propanol in the $NaNO_3$ solution were 3% w/w, 10% w/w, and 25% w/w, respectively. The propanol was selected because it does not dissolve the colloidal microsphere (unlike ethanol). Colloid solution was prepared by suspending the fluorescent microspheres (1×10^6 particle mL^{-1}) to the experimental solutions less than half hour before the initiation of experiments.

2.2. Colloidal particles and characterization

A commercial polystyrene latex microsphere (Fluoresbrite® Multifluorscent Microsphere, Polyscience, Inc., Warrington, PA) was used as the colloid tracer in the experiments. The colloids were dyed with yellow/green fluorescence and had a diameter of 980 nm and a particle density of 1.06 g cm^{-3}. The colloid concentrations were measured using a synchronous luminescence spectrometer (Perkin Elmer, LS55) by setting the constant wavelength difference ($\delta\lambda$) to 20 nm (Goeppert and Hoetzl, 2009). The maximum intensity was at an excitation wavelength of 490 nm. Calibration curves ($R^2 = 1$) obtained using the column experimental solutions were used to convert the measured intensity data to colloid concentrations. Zeta potentials of colloids were measured by ZetaPALS (Brookhaven Instrument Co.).

2.3. Steady-state saturated transport experiments

Eight transport experiments were conducted using vertical sand columns to examine the coupled effects of surface tension and ionic strength on colloid–sand interactions during steady-state saturated flow. The column was 30 cm in length and 2.05 cm in inside diameter, constructed of clear polyvinyl chloride (PVC). The setup of the column system is illustrated in Jin et al. (2000). Throughout the system, Teflon® tubing was used, except for the PVC influent fitting. Preliminary tests indicated that colloid removal by the empty column system (filled with experimental solution only) was negligible.

The column packing was initiated by pre-introducing approximately 20 mL of the background $NaNO_3$ solution of certain ionic strength and surface tension (without colloid) into the column from its bottom. Then, the dry sand was slowly poured into the solution as 1-cm increments while being stirred and tapped with a plastic rod to ensure uniformity of the packing and to avoid air entrapment in the column. The mean bulk density of the columns used in these experiments was 1.83 ± 0.02 g cm^{-3} (Table 1). The pore velocity of saturated experiments ranged between 5.5 and 6.5 cm min^{-1}, which was comparative to the averaged velocity of wetting fronts in the horizontal transient unsaturated experiments. Prior to the experiment, ~5 pore volumes (~150 mL) of the background $NaNO_3$ solution was introduced to the column using a peristaltic pump to establish a steady-state flow condition and a chemical equilibrium of the packed column with the experimental solution. Next, application of the input was switched to the colloidal suspension, which was dispersed for one minute at 10 W using a 60 sonic dismembrator (Fisher Scientific Inc.) prior to the application. After injection of approximately 5.3 pore volume (160 mL) of the colloidal suspension, the input was switched back to the background solution to elute the column under the same chemical conditions for ~4 pore volumes (~120 mL). During the course of each experiment (~40–50 min), effluent samples were collected from the top of the column into 12-mL glass test tubes with a fraction collector each 30 s. The fluorescence of the sampled colloids was then analyzed with the luminescence spectrometer. All experiments were conducted at room temperature (22 ± 1 °C) with one repetition except for Experiment #12.

2.4. Transient unsaturated transport experiments

Transient unsaturated experiments were conducted using horizontal sand columns at zero pressure head in the solutions of different ionic strengths (2, 20, and 50 mM) and surface tensions (30, 46, 54, and 73 mN m^{-1}). The column, which was pre-scored in 1-cm increments, had the same dimensions as that used for the saturated experiments. The setup of column system was illustrated in Fig. 1. Both ends of the packed horizontal column were equipped with a PVC fitting that contained a sintered stainless steel plate with an average pore size of 100 μm and a rubber gasket to seal the tube and steel plate. This allowed $NaNO_3$ solution containing

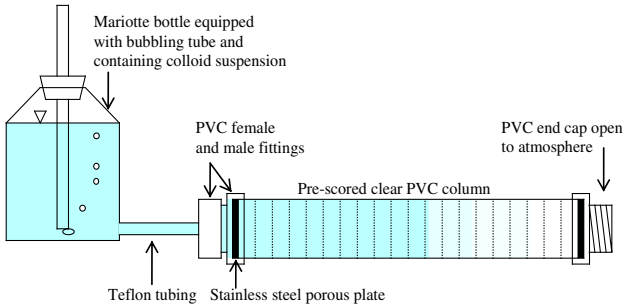

Fig. 1 – Schematic diagram of the horizontal column system.

the fluorescent microspheres (1×10^6 particle mL^{-1}) to enter the column, and air to exit the other end of the column as the solution infiltrated.

The column was packed with air-dried sand using a standard tap and fill method (Snyder and Kirkland, 1979). The colloid suspension was sonicated before it was introduced to the column from a Mariotte bottle, which was equipped with a bubbling tube for creating stable zero pressure head (Kenst et al., 2008). The zero pressure head ensured that the water flow within the column was only driven by capillary potential gradient. During the infiltration, time elapsed for the wetting front to arrive middle of each sand segment was recorded. When the colloid suspension infiltrated a distance of 26 cm into the column, the supply was terminated. This left four air-dry column segments to act as controls or for continuous moving of the liquid during sample collection. At the end of the experiment, the column was detached from the Mariotte bottle and sealed at the outlet end. The column was then immediately segmented using a pipe cutter following the procedure of Kenst et al. (2008). Each segment was weighed to determine the sand water content. The sand from each segment was then washed into 50-mL centrifuge tubes. Later, 5.0-mL of acetone (Fisher Scientific Inc., A949-4, 99% in purity) was added to each centrifuge tube and vortexed for 10 s. The colloids in the samples were then allowed to dissolve in acetone for 15 min at room temperature before a glass syringe with filter (0.2-μm pore size) was used to extract 3-mL of the dissolved colloid solution into a quartz cuvette for immediate measurement of the colloid concentrations using the luminescence spectrometer. A calibration curve was made for each experiment prior to the analysis.

3. Data analysis

For the saturated vertical transport experiments, the deposition rate of colloid on sand, K_d, was calculated by (Iwasaki, 1937; Tufenkji et al., 2003)

$$K_d = \left(\frac{v}{L}\right)\ln\left(\frac{C_0}{C_e}\right) \quad (1)$$

where v is the pore water velocity (cm min^{-1}), L the length of column (cm), C_0 the influent colloid concentration (particle L^{-1}), and C_e the maximum effluent colloid concentration (particle L^{-1}) as indicated by the plateau of breakthrough curve. Mass recovery of colloid was calculated by dividing the total number of colloids collected in the effluent at the injection and elution stages by the total number of injected colloids.

For the unsaturated horizontal transport experiments, a reverse cumulative normalized number of colloids ($\sum N_i/N_t$) was used to indicate the relative amount of colloid passing through each 1-cm sand segment as well as its variation with infiltration distance or pore water saturation (θ/θ_s). The N_i/N_t was calculated by dividing the particle number (N_i) of the colloids in the ith segment by the total particle number (N_t) of the colloids in the entire column (30 segments in total). The values of N_i/N_t were then added up starting from the last sand segment back to the inlet to obtain the reverse cumulative curves of normalized number of colloids. The curves were subsequently quantified using moment analysis method. For instance, the centroid (D_c) of the function between N_i/N_t and travel distance (D_i) in the column was identified using the following formula

$$D_c = \left(\sum_{i=1}^{30} D_i A_i\right)\left(\sum_{i=1}^{30} A_i\right)^{-1} \quad (2)$$

where A_i is the normalized mass of colloids, or fractional area under the N_i/N_t—distance curve, in the ith sand segment.

4. Results

4.1. *Effects on colloid deposition at solid-liquid interfaces*

Saturated transport experiments were conducted to examine the effects of solution surface tension and ionic strength on colloid deposition at solid–liquid interfaces. Fig. 2A shows that colloid deposition (as indicated by K_d) and mobility (as indicated by recovery percentage) at 73 mN m^{-1} were functions of solution ionic strength. The results show that deposition of colloids onto the sand surface increased with ionic strength. A threshold value of ionic strength occurred at ~20 mM, at which the colloid deposition reached its maximum (0.8 min^{-1}) while the recovery in the effluent reduced from 40% to a value as low as 3%. When the ionic strength was greater than 20 mM, colloid recovery showed no significant change with solution ionic strength.

Fig. 2B indicates a significant effect of solution surface tension on colloid recovery during transport. Decrease in surface tension from 73 mN m^{-1} to 30 mN m^{-1} increased colloid recovery by ~108 ± 6% at the three ionic strengths (2, 5, and 10 mM). This constant increase, which was independent from the magnitude of solution ionic strength, suggested that addition of low surface tension liquid (e.g., propanol) systematically changed the electric double layer interaction energies between the colloid and the sand (Batra et al., 2001). This follows according to the Derjaguin–Landau–Verwey–Overbeek (DLVO) theory (Norde and Lyklema, 1989; van Oss et al., 1999) because the zeta potential of colloids increased as solution surface tension decreased (Table 2).

4.2. *Colloid travel with wetting front*

Transient unsaturated horizontal transport experiments were conducted to examine the effects of solution surface tension

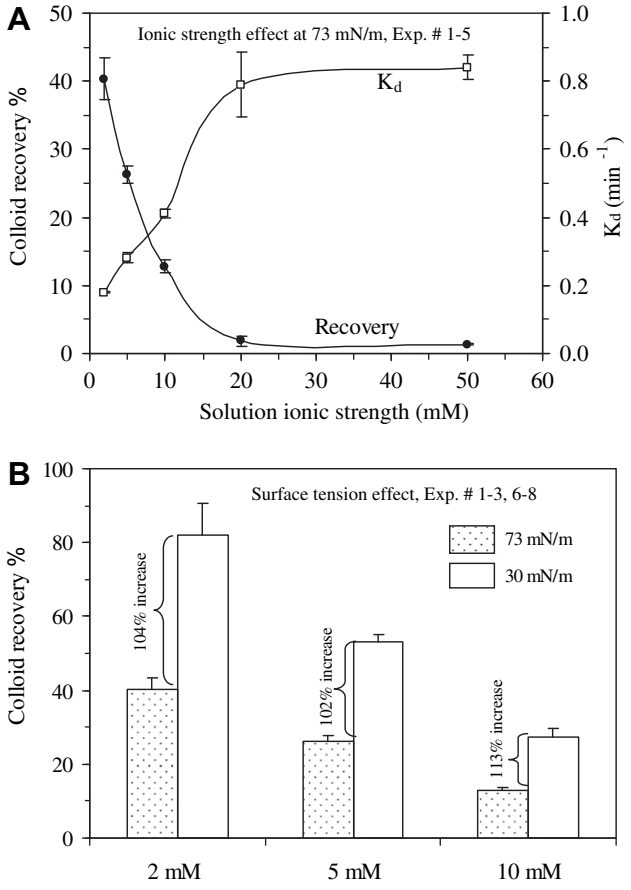

Fig. 2 – Colloid deposition (K_d) and recovery as affected by (A) ionic strength and (B) solution surface tension during the saturated transport.

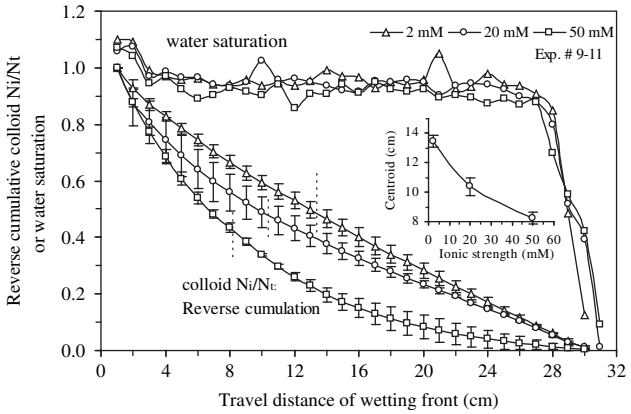

Fig. 3 – Variation of cumulative normalized colloid numbers and sand water saturation with the travel distance of wetting front in $NaNO_3$ solutions of different ionic strengths. Vertical dashed lines indicate the location of the centroids.

and ionic strength on colloid movement with capillary wetting front. Fig. 3 plots the sand water saturation (θ/θ_s) and the reverse cumulative N_i/N_t in relation to the infiltration distance (D_i). Results show that the water movement was driven by capillary force under zero pressure head and that water distribution along the column was similar at different ionic strengths. The θ/θ_s curves demonstrate that the first two segments (i.e., 0–2 cm) were fully saturated. Behind this saturated zone was a lengthening transmission zone of unsaturated flow (i.e., 3–26 cm) and fairly uniform water saturation (~90%). Beyond the transmission zone was a wetting zone, where water saturation decreased with distance down to a wetting front. At the wetting front, water moved into the dry soil and the change of saturation with distance reached largest. The last four segments (27–30 cm) were wetted due to water redistribution to the dry sand during the time of column cutting.

In contrast to the water distribution, the N_i/N_t of colloids in each segment decreased exponentially with the travel distance of the wetting front (Fig. 3). The relationship between colloid concentration and travel distance was found to be dependent on solution ionic strength. Obviously, the formed area under the curve was larger at 2 mM than at 20 mM and 50 mM, indicating that the quantity of mobile colloids had a negative relationship with the solution ionic strength. The difference between the results observed at different ionic strengths suggested that an increase in ionic strength promoted colloid retention in the sand near the inlet but decreased colloid transport to the further locations. The dashed lines indicate the centroids of the N_i/N_t versus infiltration distance functions at three ionic strengths. The centroids showed that the colloids moved farther during capillary flow as the solution ionic strength decreased (see the inset of Fig. 3).

Fig. 4A compares the effect of solution surface tension on colloid travel with wetting fronts at 2 mM and 50 mM. At both ionic strengths, decrease in solution surface tension enhanced colloid transport with capillary wetting front. Significant amount of colloids, which would be otherwise retained in the sand near the inlet of the column (i.e., colloid reservoir) in the high surface tension solution (e.g., 73 mN m^{-1}), moved farther in the solution of low surface tension (e.g., 46 mN m^{-1}), leading to a decrease in N_i/N_t in the sand near the inlet of the column but an increase in the sand far from the inlet. The surface tension effect was larger in the 2 mM solution than in the 50 mM solution. In terms of the travel distance for the center of colloid mass, the inset of Fig. 4A demonstrates that decrease in surface tension from 73 mN m^{-1} ($NaNO_3$ solution) to 30–54 mN m^{-1} (mixture of $NaNO_3$ and 2-propanol) increased the travel distance by ~126% at 2 mM, but only ~56% at 50 mM. In this study, 54 mN m^{-1} appeared to be a threshold surface tension, below

Table 2 – Zeta potential (mV) of colloids in different solutions.

Ionic strength	$NaNO_3$	$NaNO_3$ + 25% w/w 2-propanol
2 mM	−48.5 ± 1.2	−71.5 ± 5.8
20 mM	−34.4 ± 2.9	−60.7 ± 4.7
50 mM	−21.2 ± 1.1	−49.8 ± 2.9

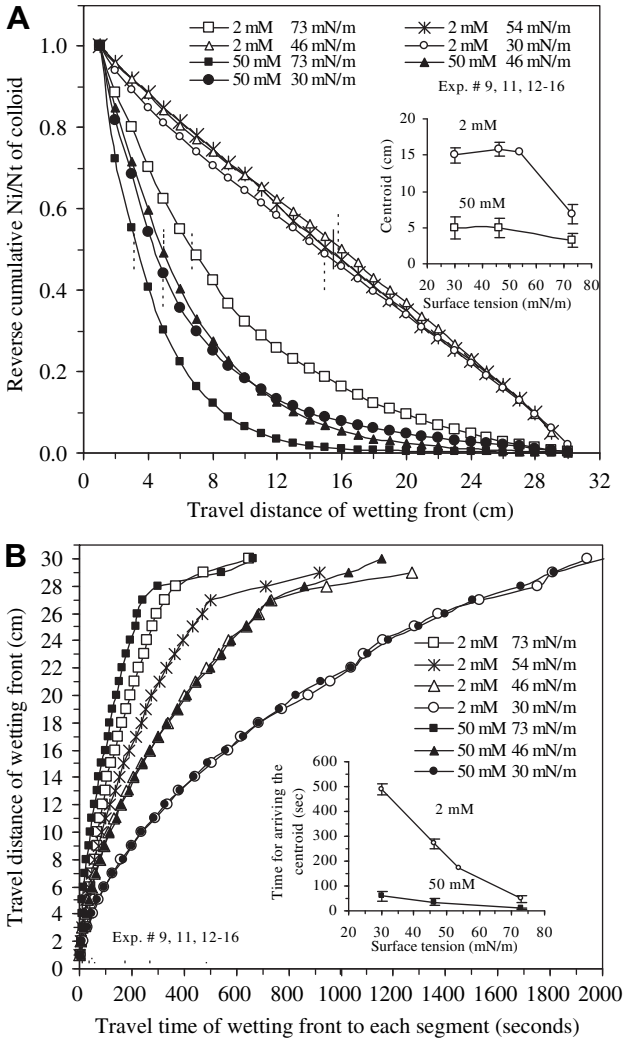

Fig. 4 – Effect of surface tension and ionic strength on (A) colloid distribution along the column and (B) the time elapsed to reach each segment during the horizontal transient unsaturated flow. Vertical dashed lines indicate the location of the centroids.

which colloid mobility did not increase significantly. These results suggested that the effect of solution surface tension on colloid transport depended on solution ionic strength and that a ~20% reduction in solution surface tension would be sufficient for gaining the maximum effect of surface tension.

In addition, surface tension affected the advancing speed of water and colloids. Fig. 4B plots the time elapsed for the wetting front to arrive in each 1-cm sand segment versus the distance between the segment and the inlet. The results showed that the travel of wetting front (also colloids) slowed down as solution surface tension decreased. The time required for the same quantity of solution and colloids to travel the same distance decreased nearly linearly with increase in solution surface tension. The linear slope was obviously much larger at 2 mM than at 50 mM, indicating increased significance of the surface tension effect on colloid travel speed at lower ionic strength.

5. Discussion

5.1. *Exponential decrease in colloid retention with travel distance*

The number of colloids in sand decreased exponentially with the travel distance of the wetting front, regardless of the uniform near-saturation (90%) of the sand in the transmission zone, which covered the most part of the column (approximately 3–26 cm). Mechanistically, the greater accumulation of colloids in the segments closer to the inlet was due to the kinetics of mass transfer of colloids from pore liquid to sand surface. Continuous influx of the colloid suspension, which passed through the sand nearer the influent end, created larger colloid flux for repeated kinetic deposition of colloids on sand, whereas the sand in farther segments was exposed to progressively smaller colloid fluxes. This observed decay of the number of colloids with travel distance was consistent with observations on the transport of a virus (φX174; 26-nm in diameter) in a similar horizontal sand column by Kenst et al. (2008). The independence of variable colloid concentrations in sand segments from uniform distribution of pore water saturation among those segments suggested that kinetic colloid deposition at solid–liquid interfaces and/or pore straining caused the exponential decay of colloid number or mass (Bradford and Bettahar, 2006). We presume that a similar trend was also associated with the saturated transport, although the saturated columns were not segmented in this study. This assumption is supported by previous studies. Kenst et al. (2008) reported that virus retention in a saturated sand column exhibited an exponential decrease in concentration or particle number with travel distance. Similarly, Torkzaban et al. (2008) observed a hyper-exponential profile of colloid deposition in vertical sand columns under both unsaturated and saturated flow conditions.

5.2. *Colloid retention at moving liquid–air interfaces*

Colloids captured at the liquid–air interfaces due to capillary forces can be mobilized when the wetting front advanced. Capillary forces are a function of colloid properties, solution surface tension, and the area of air–liquid interfaces. Since the sands in the transmission zone were near-saturated (~90%) (Fig. 3) and had little liquid–air interfaces, capillary forces might not be significant in that zone. However, capillary forces might play significant role in retaining colloids in the wetting zone, particularly bringing colloids forward at the edge of the wetting front, where the area of liquid–air interfaces reached the maximum. As illustrated by the conceptual model in Fig. 5, colloids attached at the very edge of wetting front might be first deposited at the sand surface when the sand got wetted. The number of colloids carried at the edge of a wetting front due to capillary forces, therefore, largely determined the initial deposition rate of colloids. This implies that if more colloids are associated with liquid–air interfaces at wetting fronts, greater deposition of colloids would occur as the liquid moved into the dry sand. In the study, lowering surface tension reduced capillary retention of colloids at the

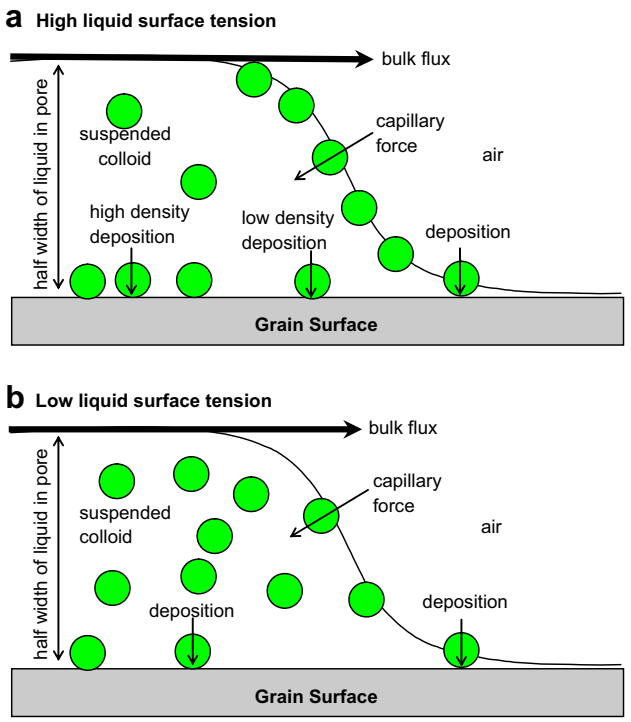

Fig. 5 – Conceptual model of colloid transport with wetting front. Note the concentrations of colloids in the liquid phase and at the solid-liquid and liquid-air interfaces are different at high and low liquid surface tensions.

liquid–air interfaces. As a result, colloids had large mobility and traveled a longer distance.

5.3. *Colloid mobility and travel velocity*

Colloid mobility can be evaluated in terms of the amount of mobilized colloids and their travel speed. The increased zeta potentials of colloids indicated that lowering solution ionic strength and surface tension increased the electrostatic repulsion between colloid and sand causing decrease in colloid deposition. Lowering liquid surface tension also resulted in less retention of colloids at the moving liquid–air interfaces particularly in the wetting zone and more suspension of colloids in the free solution, which favored more distant transport. As a result, at lower surface tension and ionic strength, more colloids were mobile. Nonetheless, decreasing solution surface tension slowed the advance of wetting front as illustrated in Fig. 4B due to reduction of capillary force for the liquid (Zartman and Bartsch, 1990; Henry et al., 1999). This reduction also caused slow migration of colloids, despite the fact that more colloids were mobile at lower solution surface tension. The shorter distances (Fig. 4A) and times (Fig. 4B) at higher ionic strength (e.g., 50 mM) suggested that the concentrations of mobile colloids in sand dominated the distance of colloid travel (or centroid of colloid mass), while the capillary movement of wetting front, which was also subject to surface tension, governed the travel velocity of colloids.

This study examined infiltration of a colloid suspension into an air-dried porous medium, which is seldom encountered in nature. However, we expect to obtain similar conclusions even in initially wet sand concerning the ionic strength effect because ionic strength mainly affects the electric double layer and may not be sensitive to change in pore water content. The only significant difference would be the decrease in infiltration rate because increasing the initial sand water content reduces the capillary driving force. In comparison, the surface tension effect may be different in initially dry and wet sands. This is because introduction of low surface tension liquid increases drainage of native sand water or lowers water retention (Zartman and Bartsch, 1990; Jawitz et al., 1998; Henry et al., 1999). The released water (high surface tension) would mix with the introduced solution (low surface tension) causing an increase in surface tension of the mixed solution. As a result, colloid retention and travel velocity would increase in initially wet relative to dry porous media. In contrast, lowering liquid surface tension might be more efficient for release or remobilization of deposited colloids from drier porous media, where colloids are usually much less mobile. Overall, the surface tension effect might be larger at low than higher water contents. This, however, needs experimental investigation.

6. Conclusions

This horizontal transport study at zero pressure head revealed a number of important phenomena concerning the coupled effects of solution surface tension and ionic strength on colloid transport during transient unsaturated flow driven by capillary forces. The main findings are:

1. Lowering solution surface tension and ionic strength decreased colloid deposition at solid-liquid interfaces due to increase in zeta potential and electrostatic repulsion;
2. The number of colloids retained in sand decreased exponentially with travel distance of the wetting front, and colloids more evenly distributed along the column as solution ionic strength and surface tension decreased;
3. Decreasing solution surface tension slowed down liquid movement and colloid travel with the wetting front due to reduction of capillary forces;
4. Surface tension effect on colloid transport was more significant at lower ionic strength;
5. Effects of solution surface tension and ionic strength on colloid deposition and transport were nonlinear. Critical threshold values appeared to exist for these two factors.

This study shows that changing solution surface tension and ionic strength can be an effective approach to controlling the distance and rate of colloid transport in porous media. The findings have significant implications for the cleanup of petroleum-associated contaminants, and are expected to improve predictions of transport of pathogens and engineered micro-fluids in different geological settings under natural unsaturated flow conditions.

Acknowledgements

This research was supported by a research project funded by Tennessee Department of Environmental Conservation and the Center for Environmental Biotechnology at the University of Tennessee. The authors appreciate the detailed comments by three anonymous reviewers.

REFERENCES

Batra, A., Paria, S., Manohar, C., Khilar, K.C., 2001. Removal of surface adhered particles by surfactants and fluid motions. AIChE J. 47 (11), 2557–2562.

Boks, N.P., Norde, W., van der Mei, H.C., Busscher, H.J., 2008. Forces involved in bacterial adhesion to hydrophilic and hydrophobic surfaces. Microbiology 154, 3122–3133.

Bradford, S.A., Bettahar, M., 2006. Concentration dependent transport of colloids in saturated porous media. J. Contam. Hydrol. 82, 99–117.

Chevalier, L., 2003. Surfactant dissolution and mobilization of LNAPL contaminants in aquifers. Environ. Monitor. Assess. 84, 19–33.

Crist, J.T., McCarthy, J.F., Zevi, Y., Baveye, P., Throop, J.A., Steenhuis, T.S., 2004. Porescale visualization of colloid transport and retention in partly saturated porous media. Vadose Zone J. 3, 444–450.

Crist, J.T., Zevi, Y., McCarthy, J.F., Throop, J.A., Steenhuis, T.S., 2005. Transport and retention mechanisms of colloids in partially saturated porous media. Vadose Zone J. 4, 184–195.

Dane, J.H., Hopmans, J.M., 2002. Pressure cell. In: Dane, J.H., Topp, G.C. (Eds.), Methods of Soil Analysis. Part 4 – Physical Methods. ASA and SSSA, Madison, WI, pp. 684–688.

DeNovio, N.M., Saiers, J.M., Ryan, J.N., 2004. Colloid movement in unsaturated porous media: recent advances and future directions. Vadose Zone J. 3, 338–351.

El-Farhan, Y.H., Denovio, N.M., Herman, J.S., Hornberger, G.M., 2000. Mobilization and transport of soil particles during infiltration experiments in an agricultural field, Shenandoah Valley, Virginia. Environ. Sci. Technol. 34, 3555–3559.

Gao, B., Saiers, J.E., Ryan, J.N., 2006. Pore-scale mechanisms of colloid deposition and mobilization during steady and transient flow through unsaturated granular media. Water Resour. Res. 42, W01410. doi:10.1029/2005WR004233.

Gao, B., Steenhuis, T.S., Zevi, Y., Morales, V.L., Nieber, J.L., Richards, B.K., McCarthy, J.F., Parlange, J.-Y., 2008. Capillary retention of colloids in unsaturated porous media. Water Resour. Res. 44, W04504. doi:10.1029/2006WR005332.

Goeppert, N., Hoetzl, H., 2009. Precise method for continuous measurement of fluorescent microspheres during flow. Hydrogeol. J.. doi:10.1007/s10040-009-0517-0 (online first).

Gomez-Suarez, C., Noordmans, J., van der Mei, H.C., Busscher, H.J. , 1999. Removal of colloidal particles from quartz collector surfaces as stimulated by the passage of liquid–air interfaces. Langmuir 15, 5123–5127.

Henry, E.J., Smith, J.E., Warrick, A.W., 1999. Solubility effects on surfactant-induced unsaturated flow through porous media. J. Hydrol. 223, 164–174.

Henry, E.J., Smith, J.E., 2002. The effect of surface-active solutes on water flow and contaminant transport in variably saturated porous media with capillary fringe effects. J. Contamin. Hydrol. 56 (3–4), 247–270.

Iwasaki, T., 1937. Dome notes on sand filtration. J. Am. Water Work Assoc. 29, 1591–1602.

Jarvis, N.J., Villholth, K.G., Ulen, B., 1999. Modeling particle mobilization and leaching in macroporous soil. Eur. J. Soil Sci. 50, 621–632.

Jawitz, J.W., Annable, M.D., Rao, P.S.C., 1998. Miscible fluid displacement stability in unconfined porous media: two-dimensional flow experiments and simulations. J. Contam. Hydrol. 31, 211–230.

Jin, Y., Chu, Y., Li, Y., 2000. Virus removal and transport in saturated and unsaturated sand columns. J. Contam. Hydrol. 43, 111–128.

Kaplan, D.I., Bertsch, P.M., Adriano, D.C., Miller, W.P., 1993. Soil-borne mobile colloids as influenced by water flow and organic carbon. Environ. Sci. Technol. 27, 1193–1200.

Kenst, A.B., Perfect, E., Wilhelm, S.W., Zhuang, J., McCarthy, J.F., McKay, L.D., 2008. Virus transport during infiltration of a wetting front into initially unsaturated sand columns. Environ. Sci. Technol. 42, 1102–1108.

Kretzschmar, R., Borkovec, M., Grolimund, D., Elimelech, M., 1999. Mobile subsurface colloids and their role in contaminant transport. Adv. Agron. 66, 121–193.

Leenaars, A.F.M., O'Brien, S.B.G., 1989. Particle removal from silicon substrates using surface-tension forces. Philips J. Res. 44, 183–209.

McCarthy, J.F., Zachara, J.M., 1989. Subsurface transport of contaminants-mobile colloids in the subsurface environment may alter the transport of contaminants. Environ. Sci. Technol. 23, 496–502.

McCarthy, J.F., McKay, L.D., 2004. Colloid transport in the subsurface: past, present, and future challenges. Vadose Zone J. 3, 326–337.

Mehra, O.P., Jackson, M.L., 1960. Iron oxide removal from soils and clays by a dithionite-citrate system buffered with sodium bicarbonate. Clays Clay Miner. 7, 317–327.

Noordmans, J., Wit, P.J., van der Mei, H.C., Busscher, H.J., 1997. Detachment of polystyrene particles from collector surfaces by surface tension forces induced by air-bubble passage through a parallel plate flow chamber. J. Adhesion Sci. Technol. 11 (7), 957–969.

Norde, W., Lyklema, J., 1989. Protein adsorption and bacterial adhesion to solid-surfaces—a colloid-chemical approach. Colloids Surf. 38, 1–13.

Ryan, J.N., Elimelech, M., 1996. Colloid mobilization and transport in groundwater. Colloid Surf. A 107, 1–56.

Ryan, J.N., Illangasekare, T.H., Litaor, M.I., Shannon, R., 1998. Particle and plutonium mobilization in macroporous soils during rainfall simulations. Environ. Sci. Technol. 32, 476–482.

Saiers, J.E., 2003. Colloid mobilization and transport within unsaturated porous media under transient-flow conditions. Water Resour. Res. 39, 1019. doi:10.1029/2002WR001370.

Saiers, J.E., Hornberger, G.M., Gower, D.B., Herman, J.S., 2003. The role of moving air–water interfaces in colloid mobilization within the vadose zone. Geophys. Res. Lett. 30, 2083. doi:10.1029/2003GL018418.

Saiers, J.E., Lenhart, J.J., 2003. Colloid mobilization and transport within unsaturated porous media under transient-flow conditions. Water Resour. Res. Lett. 39, 1019. doi:10.1029/2002WR001370.

Shang, J., Flury, M., Chen, G., Zhuang, J., 2008. Impact of flow rate, water content, and capillary forces on in situ colloid mobilization during infiltration in unsaturated sediments. Water Resour. Res. 44, W06411. doi:10.1029/2007WR006516.

Smith, J.E., Gillham, R.W., 1999. Effects of solute-concentration-dependent surface tension on unsaturated flow: laboratory sand column experiments. Water Resour. Res. 35 (4), 973–982.

Swartz, C.H., Gschwend, P.M., 1998. Mechanisms controlling release of colloids to groundwater in a Southeastern Coastal Plain aquifer sand. Environ. Sci. Technol. 32, 1779–1785.

Snyder, L.R., Kirkland, J.J., 1979. Introduction to Modern Liquid Chromatography, second ed. Wiley, New York.

Torkzaban, S., Bradford, S.A., van Genuchten, M.T., Walker, S.L., 2008. Colloid transport in unsaturated porous media: the role of water content and ionic strength on particle straining. J. Contam. Hydrol. 96, 113–127.

Tufenkji, N., Redman, J., Elimelech, M., 2003. Interpreting deposition patterns of microbial particles in laboratory-scale column experiments. Environ. Sci. Technol. 2003 (37), 616–623.

van Genuchten, M.T., 1980. A closed form equation for predicting the hydraulic conductivity of unsaturated soils. Soil Sci. Soc. Am. J. 44, 892–898.

van Oss, C.J., Norde, W., Visser, H., 1999. 50 years DLVO theory – introduction. Colloids Surf. B-Biointerf. 14, 1–2.

Walker, R.C., Hofstee, C., Dane, J.H., Hill, W.E., 1998. Surfactant enhanced removal of PCE in a partially saturated, stratified porous medium. J. Contam. Hydrol. 34, 31–46.

Wan, J.M., Wilson, J.L., 1994. Visualization of the role of the gas–water interface on the fate and transport of colloids in porous-media. Water Resour. Res. 30, 11–23.

Wan, J., Tokunaga, T., 2002. Partitioning of clay colloids at air–water interfaces. J. Colloid Interf. Sci. 247, 54–61.

Worrall, F., Parker, A., Rae, J.E., Johnson, A.C., 1999. A study of suspended and colloidal matter in the leachate from lysimeters and its role in pesticide transport. J. Environ. Qual. 28, 595–604.

Zartman, R.E., Bartsch, R.A., 1990. Using surfactants to enhance drainage from a dewatered column. Soil Sci. 149, 52–55.

Zhuang, J., Qi, J., Jin, Y., 2005. Retention and transport of amphiphilic colloids under unsaturated flow conditions: effect of particle size and surface properties. Environ. Sci. Technol. 39 (20), 7853–7859. doi:10.1021/es050265j.

Zhuang, J., McCarthy, J.F., Tyner, J.S., Perfect, E., Flury, M., 2007. In situ colloid mobilization in Hanford sediments under transient unsaturated flow conditions: effect of irrigation pattern. Environ. Sci. Technol. 41, 3199–3204.

Zhuang, J., Tyner, J.S., Perfect, E., 2009. Colloid transport and remobilization in unsaturated porous media during transient flow. J. Hydrol. 377, 112–119.